Regioselective Peroxo-Dependent Heme Alkylation in $P450_{BM3}$-F87G by Aromatic Aldehydes: Effects of Alkylation on Catalysis†

Gregory M. Raner,* James A. Hatchell, Montegue U. Dixon, Teresa L. Joy, Alice E. Haddy, and Eric R. Johnston

Department of Chemistry and Biochemistry, The University of North Carolina at Greensboro, Greensboro, North Carolina 27402-6170

Received April 1, 2002; Revised Manuscript Received May 30, 2002

ABSTRACT: Cytochrome $P450_{BM3}$-F87G reacts with aromatic aldehydes and hydrogen peroxide to generate covalent heme adducts in a reaction that may involve the formation of a stable isoporphyrin intermediate [Raner, G. M., Hatchell, A. J., Morton, P. E., Ballou, D. P., and Coon, M. J. (2000) *J. Inorg. Biochem. 81,* 153−160]. Electron paramagnetic resonance spectra for the proposed isoporphyrin intermediates generated using two different aromatic aldehydes suggest that, in each case, the heme remained coordinated to the apoenzyme via the cysteine thiolate, the metal center remained ferric low spin, and a slight distortion in the geometry of the pyrrole nitrogens occurred. Characterization of the resulting heme adducts via 1D and 2D NMR showed conclusively that the heme was modified at the γ-meso position alone, and mass spectral analysis indicated loss of formate from the aldehyde prior to alkylation. The enzyme derivatives in which the hemes were covalently altered retained the characteristic UV/vis and EPR spectral properties of a P450, indicating that the heme was properly ligated in the active site. The modified enzymes were able to accept electrons from NADPH in the presence of lauric acid at a rate comparable to that of the unmodified forms, although oxidation of the lauric acid was not observed with either modified enzyme. Oxidation of 4-nitrophenol and 4-nitrocatechol was observed for both derivatives. However, 4-nitrocatechol oxidation was completely quenched in the presence of superoxide dismutase. The results are consistent with heme modification occurring through a peroxo-dependent pathway and also suggest that modification results in altered catalytic activity, rather than complete inactivation of the P450.

Aldehydes are known to reduce detectable levels of cytochrome P450 enzymes in rat liver microsomes (*1*), while in a reconstituted system a variety of aldehydes have been shown to be potent mechanism-based inactivators of certain rabbit liver isoforms (*2*). The cytochrome P450-dependent formation of a reactive alkyl radical, with subsequent attack of this radical at the enzyme's heme prosthetic group, has been implicated in the destructive effects of aldehydes on microsomal P450 isoforms (*3*). Structural features that appear to influence the destructive power of the aldehyde are α,β-unsaturation and branching in the α-position. With certain aldehydes, the heme group is completely destroyed, whereas with others, an alkyl-heme derivative appears to be very stable. It is unclear whether the enzymes possessing the covalently modified heme retain any catalytic activity.

In a recent study, cytochrome $P450_{BM3}$-F87G was shown to catalyze the peroxide-dependent deformylation of aromatic aldehydes in a reaction that resulted in the covalent modification of the heme prosthetic group of the enzyme (*4*). The reaction was monitored by stopped-flow spectrophotometry and appeared to involve the proposed P450 peroxo pathway. The only observable intermediate in this reaction had a λ_{max} of 430 nm, a lower extinction coefficient than that of the starting heme or the resulting heme adduct, and was stabilized by branching in the parent aldehyde. The spectral properties of this intermediate led to its identification as an isoporphyrin, in which a heme meso-carbon was converted from an sp^2- to an sp^3-hybridized carbon. A similar intermediate has been reported for heme modification involving horseradish peroxidase (*5*, *6*) and myoglobin (*7*). Subsequently, the isoporphyrin underwent deprotonation, resulting in the observed meso-alkyl-substituted heme, which was characterized by electronic absorption spectrophotometry and atomic absorption spectroscopy. Although no NMR analysis was reported, comparison of the spectral data to that obtained in an earlier study involving $P450_{2B4}$, in which NMR and mass spectrometry were used, suggested a similar heme structure in the BM3-F87G[1] experiments (*8*).

The wild-type cytochrome $P450_{BM3}$ is a fatty acid hydroxylase with a very high degree of regio- and stereoselectivity. However, it has been reported that mutation of Phe-87 altered the selectivity of the enzyme, due to removal of a steric barrier within the active site (*9*). Furthermore, the F87A mutant was shown to be more effective in the oxidation of *p*-nitrophenoxycarboxylic acids than the wild-

† This investigation was supported by a Cottrell College Research Award (Grant CC4924) from the Research Corporation and The University of North Carolina at Greensboro.

* To whom correspondence should be addressed: tel, (336) 334-4519; fax, (336) 334-5402; e-mail, gmraner@uncg.edu.

[1] Abbreviations: $P450_{BM3}$, cytochrome $P450_{BM3}$; 3PP, 3-phenylpropionaldehyde; 3PB, 3-phenylbutyraldehyde; NOE, nuclear Overhauser effect; BM3-F87G, cytochrome $P450_{BM3}$ with Phe-87 mutated to Gly; F87G-3PP, the F87G mutant of $P450_{BM3}$ in which the heme was modified using 3PP; F87G-3PB, the F87G mutant of $P450_{BM3}$ in which the heme was modified using 3PB.

10.1021/bi020256c CCC: $22.00
Published on Web 07/04/2002

type enzyme, suggesting that the open space provided by elimination of the aromatic side chain at position 87 allowed improved access of aromatic substrates to the active site (*10*). In addition, several other groups have shown that mutations in the active site can result in BM3 mutants with substantial activity toward aromatic substrates (*11*, *12*).

In the current study, we have further examined the putative isoporphyrin intermediate generated in the reaction of either 3-phenylbutyraldehdye or 3-phenylpropionaldehyde with $P450_{BM3}$-F87G, in the presence of hydrogen peroxide. We have done this by trapping the intermediate using liquid nitrogen and subsequent analysis by electron paramagnetic resonance (EPR) spectroscopy. In the previous study by Raner et al. (*4*) it was concluded that the γ-meso position was the site of attachment, based on the assumption that the aldehyde phenyl group occupied the region of the active site that was made available by the mutation of Phe-87, and this site was adjacent to the γ-meso carbon. In addition, differences in the rates of deprotonation of the proposed isoporphrin intermediates generated with 3PP and 3PB suggested the addition was to a sterically hindered position on the heme, which was consistent with the γ-position. In the present study the alkylated hemes generated as products of this reaction have been purified and subjected to analysis by 1D and 2D NMR in an effort to confirm this assignment. Finally, the catalytic properties of the enzymes containing covalently altered hemes have been determined using the substrates lauric acid, 4-nitrophenol, and 4-nitrocatechol. Product formation and NADPH consumption rates have been monitored and compared to the rates observed for wild type and the F87G mutant of $P450_{BM3}$.

EXPERIMENTAL PROCEDURES

Chemicals. The compounds 3-phenylpropionaldehyde and 3-phenylbutyraldehyde were purchased from Sigma-Aldrich, along with NADPH, IPTG, heme, and the substrates 4-nitrophenol and 4-nitrocatechol. [^{14}C]Lauric acid was obtained from Novartis Crop Protection (Greensboro, NC). Buffers and media reagents were purchased from Fisher Scientific and were of the highest grade available.

Enzyme Preparation. *Escherichia coli* cells expressing wild-type and the F87G mutant cytochrome $P450_{BM3}$ were a gift from Dr. David Mullen (Tulane University, New Orleans, LA). The cells were grown and induced according to the method described by Raner et al. (*4*). The purification of $P450_{BM3}$ and BM3-F87G has also been reported in the literature (*4*). Enzyme concentrations were calculated on the basis of the method of Omura and Sato (*13*) using an extinction coefficient of 91000 cm^{-1} M^{-1} at 450 nm for the reduced vs reduced − CO difference spectrum. The enzyme samples used for heme extraction and NMR analysis were purified by a slightly different procedure in an attempt to optimize the yield of enzyme. Following cell lysis and centrifugation, the clarified sample was subjected to anion-exchange chromatography on a DE-52 column equilibrated in 50 mM phosphate buffer (pH 7.4) containing 15% glycerol. After the column was washed with 10 volumes of this same buffer, the protein was eluted by the addition of 0.15 M NaCl to the wash buffer. The P450 eluted from the column under these conditions as the major protein component in the sample, as determined by SDS−PAGE.

Preparation of Heme Samples for NMR Analysis. Native iron protoporphyrin IX was purchased from Sigma Chemical Co. for use as a control in the NMR studies. Approximately 1.0 μmol was dissolved in 0.5 mL of pyridine-d_5, and the sample was reduced under nitrogen using stannous chloride. The modified hemes were prepared using a variation of the methods used by Raner et al. and Kuo et al. (*4*, *8*). Enzyme samples, in 100 mM phosphate buffer, pH 7.4, containing 15% glycerol, were diluted to a final concentration of 5−10 μM in a reaction mixture containing 2.5 mM aldehyde, 100 mM phosphate, pH 7.4, and ~2.5 mM H_2O_2. The reaction was carried out at 7 °C for 30−60 min with constant mixing, after which the enzyme was diluted 1:5 with 50 mM phosphate buffer (pH 7.4) and 15% glycerol and then loaded onto a DE-52 ion-exchange column equilibrated in 50 mM phosphate buffer (pH 7.4) at 7 °C. After the column was washed with 5 column volumes of equilibration buffer to remove aldehyde and H_2O_2, the enzyme was eluted using the equilibration buffer containing 0.400 M NaCl. To these enzyme samples was added 0.5% glacial acetic acid, which resulted in precipitation of the enzyme. The denatured sample was then centrifuged, and the supernatant, which contained the flavin from the reductase domain, was discarded. The pellet contained greater than 90% of the heme from the enzyme sample. The pellet was treated with acetonitrile containing 0.1% TFA for 16 h at −20 °C in the dark, which resulted in the efficient extraction of the heme from the protein pellet. This procedure was repeated two more times to maximize the yield. The combined samples were then diluted with distilled water to a final composition of 35:65 acetonitrile:H_2O, and TFA was added in sufficient quantity to produce a 0.1% mixture. The sample was applied to a Whatman solid-phase extraction column (200 mg, C-18) to concentrate and remove residual protein. After being washed with 10 column volumes of 0.1% TFA, the heme sample was eluted in 100% methanol containing 0.1% TFA. Following evaporation of the methanol, the sample was taken up in 60:40 acetonitrile:H_2O containing 0.1% TFA and submitted to HPLC purification using a C-18 reversed-phase column. The purified sample was again applied to a solid-phase extraction cartridge and eluted as described above.

Electrospray Mass Spectral Analysis. A sample of the heme that was modified with 3PP and dissolved in methanol was analyzed by direct infusion into an LCQ advantage ion trap mass spectrometer operating in the positive ion mode at a flow rate of 250 μL/min. The final heme concentration for this analysis was 20 μM.

NMR Measurements. The purified heme sample in methanol was taken to dryness, redissolved in D_2O in the presence of 5 μL of triethylamine, and dried again under reduced pressure at 45 °C. This procedure was repeated two more times. The heme was dissolved in 300 μL of pyridine-d_5, and 50 mg of $SnCl_2$ was dissolved in 200 μL of the same solvent in a separate vial. Each sample was purged repeatedly by a freeze/thaw cycle under reduced pressure. The two mixtures were then combined in an NMR tube under an argon atmosphere. Additional pyridine-d_5 was added to bring the volume to 700 μL. The final concentrations of the heme samples were 1.1 and 0.97 mM for 3PB and 3PP, respectively. Concentrations were determined using an extinction coefficient of 104000 M^{-1} cm^{-1} at 408 nm, as reported previously (*4*).

Experiments were carried out using a Bruker Avance 300 NMR spectrometer equipped with an inverse probe, operating at an ^{1}H frequency of 300.13 MHz. The instrument was programmed with a delay time of 1.3 s and a mixing time of 300 or 800 ms. Processing of the spectra was performed on an Indy Silicon Graphics data station. NOESY spectra were obtained with 1K data points in the t_2 dimension and a 1K block of 128 scans, each in the t_1 dimension. Free induction decays were zero-filled once in both dimensions and apodized with a sine function.

EPR Experiments. EPR samples were prepared by combining P450 (20 μM) with the aldehyde (2.5 mM) and H_2O_2 (1−3 mM) at 0 °C in 80 mM phosphate buffer, pH 7.4. At various reaction times ranging from 1 to 60 min, 1.0 mL samples were removed and rapidly frozen in EPR tubes using liquid nitrogen. Control samples were prepared in which either H_2O_2 alone or H_2O_2 and aldehyde were left out. Spectra were recorded using a Bruker Model EMX 6/1 EPR spectrometer at a microwave power of 0.504 mW and a frequency of 9.482 GHz. All spectra were taken at 10 K, and the temperature was controlled using an Oxford Instruments ESR 900 cryostat.

Catalytic Activities of the Native and Modified Enzymes. Enzyme purification and heme modification were carried out as described previously in this paper. The enzymes modified using 3PP and 3PB were analyzed by HPLC in an attempt to determine accurate enzyme concentrations. A 50 μL aliquot of each modified enzyme sample was injected onto a C-18 RP-HPLC column under the isocratic solvent conditions of 60:40 acetonitrile:H_2O containing 0.1% TFA. The heme peaks were integrated, and the areas were compared to the area of known amounts of native heme. The extinction coefficient of the modified enzyme is not significantly different from that of the native heme.

The rates of NADPH oxidation by wild-type P450$_{BM3}$, BM3-F87G, F87G-3PP, and F87G-3PB were measured using a High-Tech Model SFA-11 stopped flow, connected to an HP-8452 diode array spectrophotometer. One syringe contained a solution of 0.40 μM enzyme and 0.80 mM lauric acid in 100 mM phosphate buffer, pH 7.4. The other syringe held a solution of 2.0 mM NADPH in 100 mM phosphate buffer, pH 7.4, also containing 0.80 mM lauric acid. The two solutions were mixed in equal proportions at 37 °C, and the rate of NADPH oxidation was determined by monitoring absorbance changes at 340 nm. Rates were determined over the initial 5 s of the reaction, and experiments were carried out in multiples of five or more. A minimum of 20 trials were performed with each of the four different forms of the enzyme.

The ability of wild-type P450$_{BM3}$, BM3-F87G, F87G-3PP, and F87G-3PB to affect the oxidation of three different substrates was also assessed. First, hydroxylation of ^{14}C-labeled lauric acid was measured. Reaction mixtures consisted of 0.20 μM P450, 0.10 mM lauric acid with a specific activity of 8.4 mCi/mmol, 100 mM phosphate buffer, pH 7.4, and 1.0 mM NADPH. The reactions were carried out for 10 min at 37 °C, after which the protein was precipitated by addition of 0.4 volume of 6% perchloric acid. Following centrifugation, 50 μL of the supernatant was injected on a C-18 RP-HPLC column with a mobile phase of 60:40 acetonitrile:H_2O. The hydroxylated product was detected using an IN/VS β-RAM radiomatic flow detector. The oxidation of 4-nitrophenol was carried out as described in the literature (*14*) except that the substrate concentration was varied between 1.0 and 10.0 mM and the reactions were quenched with 6% perchloric acid following a 10 s incubation. The rate of oxidation of 4-nitrocatechol by the wild-type, P450$_{BM3}$-F87G, and its two covalently modified forms was determined as follows: Reaction mixtures consisted of 0.1−0.5 mM 4-nitrocatechol and 1.0 mM NADPH in 100 mM phosphate buffer at pH 7.9. The reactions were carried out for 4 min at 37 °C in a water bath, quenched by addition of 0.4 volume of 6% perchloric acid, and centrifuged to remove precipitated material. All assays were performed in duplicate, and samples were injected onto a C-18 HPLC column using a previously described HPLC system (*4*) with an isocratic mobile phase of 65% H_2O and 35% acetonitrile (containing 0.1% TFA) at a flow rate of 1.0 mL/min, with detection at 350 nm. Identical experiments involving aromatic substrates were also carried out in the presence of 250 units of catalase, 250 units of SOD, or 250 units of both.

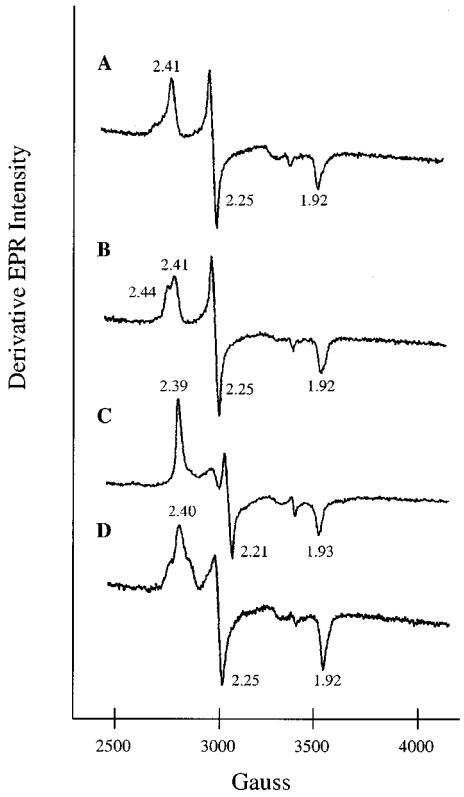

FIGURE 1: EPR spectra at 10 K for (A) BM3-F87G, (B) BM3-F87G in the presence of 2.5 mM 3-phenylbutyraldehyde, (C) as in (B) but following 10 min incubation with aldehyde and 3.0 mM H_2O_2 at 0 °C, and (D) as in (B) but following a 30 min incubation with aldehyde and H_2O_2 at 22 °C. All samples contained 20 μM P450, 100 mM phosphate buffer at pH 7.4, and 15% glycerol.

RESULTS

EPR Characterization of the Intermediate Formed in the Reaction with Aromatic Aldehydes and Hydrogen Peroxide. Cytochrome P450$_{BM3}$-F87G was purified to homogeneity, and the EPR spectrum of the purified enzyme was recorded. The spectrum in Figure 1A shows the characteristic signal for a low-spin, ferric cytochrome P450 enzyme, with *g*-values of 1.92, 2.25, and 2.41 (*15*). Upon addition of 2.5 mM 3-phenylbutyraldehyde, the component of the EPR signal centered at 2.41 split into two signals, one with $g = 2.41$

Table 1: Observed *g*-Values in the EPR Spectra for Various BM3-F87G Complexes during Reaction with H_2O_2 and Aldehydes

aldehyde	enzyme form	*g*-values
none	Fe(III)	2.41, 2.25, 1.92
3PB[a]	Fe(III)	(2.44, 2.41), 2.25, 1.92
	intermediate	2.39, 2.21, 1.93
	Fe(III) modified	(2.44, 2.41, 2.39), 2.25, 1.92
3PP[a]	Fe(III)	(2.44, 2.41), 2.25, 1.92
	intermediate	2.40, 2.22, 1.93
	Fe(III) modified	(2.40, 2.37), 2.26, 1.92

[a] Numbers in parentheses indicate that this component of the signal was split.

and the other with $g = 2.44$ (Figure 1B). The sample was treated with 3.0 mM H_2O_2 (final concentration) at 0 °C for 10 min and frozen in liquid nitrogen, with the resulting spectrum shown in Figure 1C. This intermediate was characterized by a signal with *g*-values of 1.93, 2.21, and 2.39. The spectrum shown in Figure 1D was recorded for a sample that had been treated in an identical manner, except that, following the addition of H_2O_2, the reaction mixture was incubated at room temperature for 30 min. The same experiment was carried out using 3PP instead of 3PB, and results for the second aldehyde were very similar to the first. In each case an intermediate was observed with the $g = 2.25$ component shifting to $g = 2.21$, and upon being allowed to stand at room temperature, the $g = 2.21$ component returned to its starting position of $g = 2.25$ while the low-field component remained split. The only notable difference was that, with 3PB modification, the low-field component was split into three peaks, while 3PP modification resulted in two peaks. The *g*-values for both sets of spectra are summarized in Table 1.

Spectroscopic Analysis of the Modified Hemes Produced in the Reaction with Aldehyde and Hydrogen Peroxide. Semi-purified cytochrome $P450_{BM3}$-F87G (described in Experimental Procedures) was combined with either 3PP or 3PB, along with hydrogen peroxide, and the reaction was monitored using UV/vis spectrophotometry. The heme modification was characterized by a shift in the enzyme Soret maximum from 418 to 430 nm, as previously reported (*4*). The resulting modified hemes were removed from the protein and purified by HPLC. Electronic absorption spectra of the two hemes were also recorded and were consistent with those reported by Kuo et al. in a study involving the 2B4 isoform (*8*). Each displayed a λ_{max} at 408 nm, consistent with meso-heme addition by an alkyl group (data not shown). Mass spectral data for the 3PP-modified heme indicated a molar mass of 719.5 Da, compared to 615.5 Da for the wild-type heme.

The NMR spectrum of the reduced 3PP modified heme in pyridine-d_5 is shown in Figure 2. Of particular interest are the proton signals between 9 and 10 ppm, which correspond to the meso protons of the heme. In this spectrum, only three meso protons could be observed in the region between 9 and 10 ppm. With the 3PB-modified heme, many of the proton signals appeared to be split, as indicated by Figure 3, which shows the 1D NMR spectrum for this derivative. The spectrum was very complex, relative to the 3PP spectrum, due to the splitting, which did not appear to be consistent with simple scalar coupling. Two of the meso protons appeared as doublets, while one appeared as a singlet,

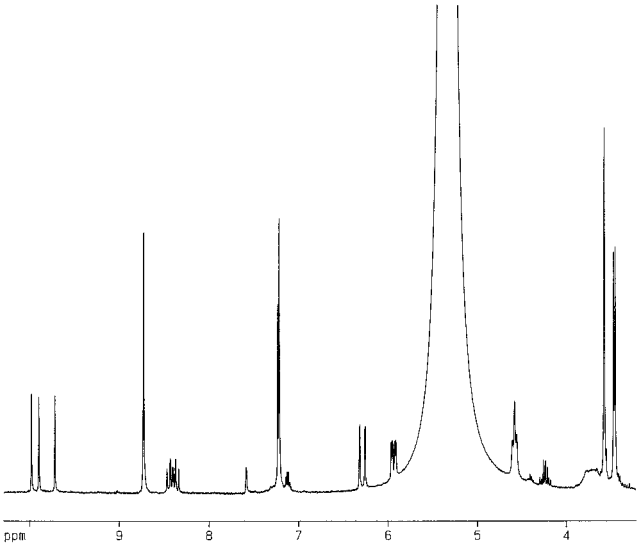

FIGURE 2: NMR spectrum of the purified heme adduct generated in the reaction of BM3-F87G with 2.5 mM 3-phenylpropionaldehyde and 2.5 mM H_2O_2. The reaction was carried out in 100 mM phosphate buffer, pH 7.4, containing 15% glycerol for 30 min between 4 and 8 °C.

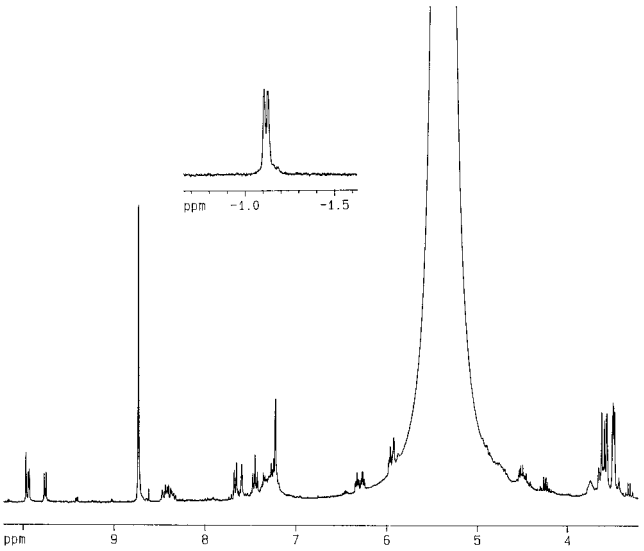

FIGURE 3: NMR spectrum of the purified heme adduct from the reaction of BM3-F87G with 2.5 mM 3-phenylbutyraldehyde and 2.5 mM H_2O_2. The reaction was carried out in 100 mM phosphate buffer, pH 7.4, containing 15% glycerol for 30 min between 4 and 8 °C. The aldehyde used for this experiment was a mixture of the (*R*) and (*S*) enantiomers, which may explain the splitting of many of the proton signals. The signal at −1.20 ppm was not observed in the 3-phenylpropionaldehyde spectrum and has therefore been assigned to the branching methyl group on the aldehyde.

and integration of the meso proton signals in this spectrum indicated a 1:1:1 ratio. The aldehyde 3-phenylbutyraldehyde contains a single chiral center, and the parent aldehyde used in the modification reaction was an enantiomeric mixture. It would appear that the splitting of nearly all of the proton signals in the NMR spectrum of this heme was the result of the presence of two isomeric forms of the modified heme.

Assignment of the meso proton signals for the 3PP-modified sample was straightforward using two-dimensional NMR analysis. The NOE interactions between the meso protons and the methyl protons are illustrated in Figure 4A. Interactions could be observed between the meso proton at

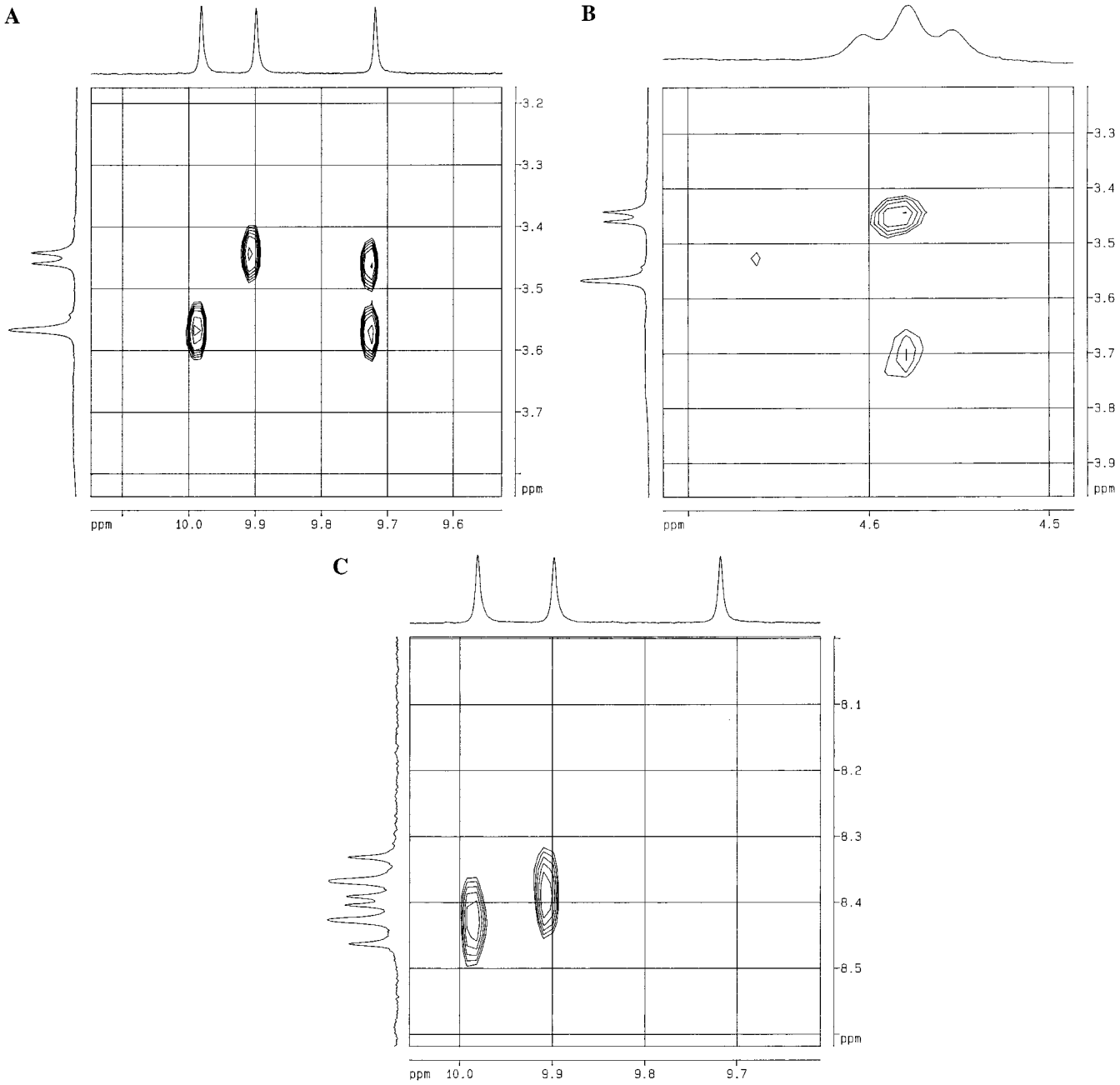

FIGURE 4: NOESY regional maps of the heme adduct formed in the H_2O_2-dependent reaction of BM3-F87G with 3-phenylpropionaldehyde. The interaction between the meso and methyl protons is shown in panel A, the interaction between methyl protons and α-propionic acid protons is shown in panel B, and the interaction between methyl and vinyl protons is shown in panel C.

9.71 ppm and two sets of methyl protons at 3.44 and 3.57 ppm. Cross-peaks were also observed for the meso proton at 9.89 ppm and the methyl signal at 3.46 ppm, as well as for the meso proton at 9.98 ppm and the methyl signal at 3.57 ppm. On the basis of the integration of the methyl proton signals, the peak at 3.57 ppm corresponded to two distinct sets of methyl protons with the same chemical shift. Figure 4B shows the 2D NMR spectrum in the region of the methyl protons and the α-propionic acid protons, and Figure 4C illustrates the interactions between vinyl groups and the meso protons. The observed NOE interactions for the 3PP-modified heme used in this study are summarized in Table 2. Similarly, the meso protons of the 3PB-modified enzyme showed NOE interactions with several methyl groups (Figure 5). In particular, the meso proton corresponding to a doublet signal centered at 9.76 ppm showed cross-peaks with two distinct methyl signals. The two remaining meso protons each interacted with a single methyl group. The complexity of the spectrum, due to the presence of two stereoisomers of the 3PB-modified heme, made complete assignment of all the methyl signals impossible.

Table 2: NMR Chemical Shifts and NOESY Interactions of the 3-Phenylpropionaldehyde Heme Adduct

proton	chemical shift (ppm)	interaction
α-meso	9.980	3-methyl
β-meso	9.898	5-methyl
δ-meso	9.718	1-methyl, 8-methyl
1-methyl	3.567	*δ*-meso
3-methyl	3.567	α-meso
5-methyl	3.442	α-propionic, *δ*-meso
8-methyl	3.460	α-propionic, *β*-meso

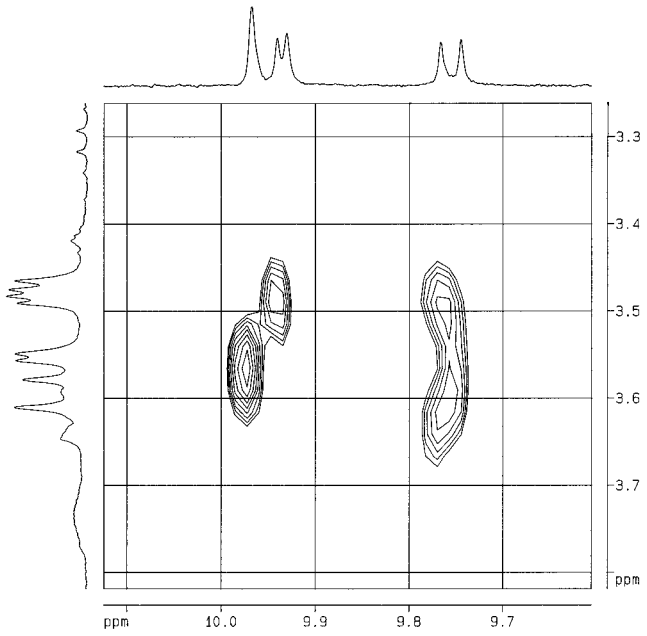

FIGURE 5: NOESY regional map of the heme adduct formed in the H_2O_2-dependent reaction of BM3-F87G with 3-phenylbutyraldehyde. The interaction between the methyl protons and the meso protons is shown.

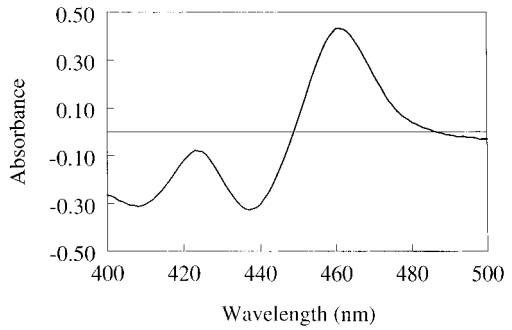

FIGURE 6: Reduced − CO difference spectrum for the covalently modified F87G-3PB enzyme. The sample was prepared as described in Experimental Procedures, and the spectrum was recorded at room temperature in 100 mM phosphate buffer, pH 7.4. The spectrum was recorded ~10 s after addition of dithionite to the sample. Subsequent scans showed a decrease in the 460 nm absorbance with a corresponding increase at 424 nm, suggesting the reduced − CO complex was unstable under these conditions.

Catalytic Properties of the Modified Enzyme. Heme modification via the peroxo pathway did not lead directly to loss of heme by the enzyme. For example, following treatment with 3PB (or 3PP) and hydrogen peroxide, the enzyme could be further purified by ion-exchange chromatography in order to remove excess aldehyde and peroxide and still retained its spectrophotometric properties. Whereas the unmodified enzyme showed a λ_{max} for the reduced vs reduced − CO difference spectrum of 450 nm, the λ_{max} for the modified enzyme was 460 nm (Figure 6). Furthermore, in the presence of the substrate lauric acid, the enzymes modified with both 3PP and 3PB retained their ability to accept electrons from NADPH, as determined by NADPH consumption assays. The initial rates of NADPH consumption by 3PP- and 3PB-modified BM3-F87G, along with unmodified BM3-F87G and the wild-type enzyme, are summarized in Table 3. According to the data, the enzymes had NADPH consumption rates of 1203 and 1094 nmol min^{-1} $nmol^{-1}$ for the 3PB- and 3PP-modified forms, respectively, which were similar to that of the unmodified form (1230 nmol min^{-1} $nmol^{-1}$). All three were about 50% as active as the wild-type enzyme (2663 nmol min^{-1} $nmol^{-1}$) under identical conditions. Although reactions were monitored for 1 min, the rates were calculated on the basis of the initial 5 s of the reaction. This is because the kinetics were not linear over the full 1 min. In fact, at the end of 1 min, the enzymes all appeared to be virtually inactive. Although the initial rates of the two modified forms appeared to be similar, they appeared to be more susceptible to turnover-dependent inactivation so their rates of catalysis dropped off more sharply than the unmodified forms.

Table 3: NADPH Consumption Rates for the Wild-Type, F87G Mutant, and F87G-3PP and F87G-3PB Forms of $P450_{BM3}$

enzyme	turnover number [nmol min^{-1} (nmol of P450)$^{-1}$]
$P450_{BM3}$	2663 ± 178
BM3-F87G	1230 ± 74
F87G-3PP	1094 ± 64
F87G-3PB	1203 ± 102

The ability of the F87G, and modified forms, to catalyze fatty acid oxidation was examined using ^{14}C-labeled lauric acid as a substrate. Wild-type BM3 catalyzed this reaction very efficiently. For example, following a 10 min incubation in the presence of 0.2 μM wild-type enzyme, 100% of the ^{14}C-labeled lauric acid was converted to more polar metabolites. Under the same conditions, the F87G mutant converted only 17% of the lauric acid to products. Increasing lauric acid or NADPH concentration did not affect the amount of product formed in this reaction, though the amount of lauric acid oxidized did increase with increasing amounts of enzyme. The products formed in the reactions of both wild-type and F87G had identical retention times of 45.5 min under the HPLC conditions employed, compared with 55.0 min for lauric acid, but we could not confirm the regio- or stereoselectivity of the enzymes. When the experiment was carried out using the F87G-3PP or F87G-3PB derivatives, no product or decrease in ^{14}C-labeled lauric acid was observed.

Cytochrome $P450_{BM3}$ can affect the oxidation of 4-nitrophenol, and the product of this reaction, 4-nitrocatechol, can be further oxidized to 2,3,4-trihydroxynitrobenzene as determined by NMR and MS analysis (unpublished experiments). Both reactions require NADPH and O_2. In the current study, we have shown that the covalently modified forms of the enzyme were as active in carrying out the oxidation of 4-nitrocatechol as the unmodified form, consistent with the results involving NADPH oxidation rates. However, oxidation of the 4-nitrocatechol was inhibited in the presence of SOD and catalase (Table 4). Subsequent experiments showed that the SOD completely eliminated 4-nitrocatechol oxidation, whereas the effect of catalase on this activity was modest (Figure 7). In contrast, the oxidation of 4-nitrophenol was not dramatically affected by either SOD or catalase as indicated in Table 4. If anything, this activity increased slightly in the presence of SOD and catalase. The oxidation of 4-nitrophenol by the modified enzymes occurred with a lower catalytic efficiency than with the unmodified F87G mutant. The reduced efficiency was primarily the result of k_{cat} values that were less than one-fifth that of the F87G,

Table 4: Catalytic Activities of Different Forms of P450$_{BM3}$

	4-nitrophenol oxidation[a]		4-nitrocatechol oxidation[b]
reaction	K_m (mM)	k_{cat} (nmol min^{-1} nmol^{-1})	velocity (nmol min^{-1} nmol^{-1})
wild type	16 ± 5	22 ± 6	11.4 ± 2
SOD and catalase	22 ± 9	29 ± 9	0.0
F87G	2.8 ± 0.4	42.8 ± 2.6	52.6 ± 2.6
SOD + catalase	3.1 ± 0.3	45.0 ± 2.1	0.0
F87G-3PP	2.7 ± 1.0	8.1 ± 1.0	76.1 ± 4.0
SOD + catalase	4.1 ± 0.6	8.2 ± 0.7	0.0
F87G-3PB	1.0 ± 0.2	4.6 ± 0.3	35.5 ± 1.8
SOD + catalase	1.5 ± 0.5	6.0 ± 0.7	0.0

[a] The product 4-nitrocatechol was monitored after a 10 s incubation at 37 °C. [b] Activity was measured at pH 8.0 using a 4.0 min incubation at 37 °C and a substrate concentration of 100 μM.

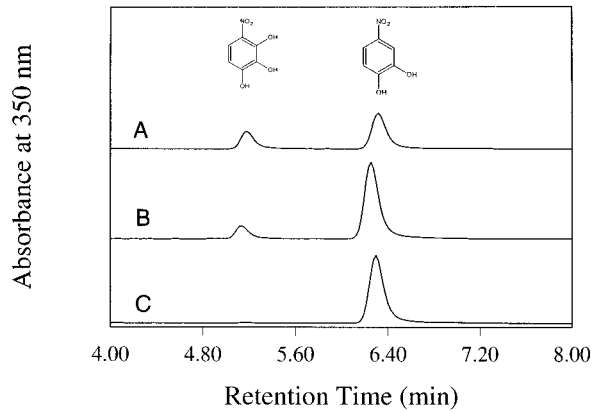

FIGURE 7: A portion of the HPLC chromatograms showing the effects of catalase and SOD on the BM3-F87G-catalyzed oxidation of 4-nitrophenol and subsequent oxidation of the product 4-nitrocatechol. The reactions were carried out for 20 min at 37 °C. Samples consisted of (A) 0.5 μM BM3-F87G, 2.5 mM 4-nitrophenol, 100 mM phosphate buffer, pH 7.4, and 1.0 mM NADPH, (B) same as (A) with addition of 250 units of catalase, and (C) same as (A) with addition of 250 units of SOD. Under these conditions, 4-nitrophenol had an HPLC retention time of 9.1 min.

while K_m values were comparable. It is worth noting that the wild-type enzyme was a less efficient oxidizer of 4-nitrophenol than the F87G mutant, as indicated by a 6-fold increase in K_m and ~50% reduction in k_{cat}.

Time course experiments were carried out using the F87G mutant and F87G-3PP to establish the linearity of the reaction involving 4-nitrophenol. Consistent with the NADPH oxidation results, the reaction rate decreased with time for both enzymes; however, the F87G-3PP derivative was particularly sensitive to inactivation. For example, within 20 s, the F87G mutant was reduced to 50% activity, while over the same period of time, F87G-3PP retained ~25% of its activity.

DISCUSSION

In the previous studies by Raner et al. (*4*), an isoporphyrin species was proposed as an intermediate in the reaction of cytochrome P450$_{BM3}$-F87G with aromatic aldehydes and hydrogen peroxide. This assignment was based on the observed decrease in the extinction coefficient of the Soret peak and the appearance of an absorption peak in the 700−900 nm region. We have examined this intermediate using EPR in an attempt to further characterize this species. At low temperatures (0−12 °C), the intermediate appeared to be much more stable than at 22 °C and did not readily convert to the final product. This greatly facilitated the preparation of samples for EPR analysis. The use of both 3PP and 3PB resulted in the formation of intermediates with very nearly identical EPR spectra.

The general shape and *g*-values associated with the EPR signal of this intermediate indicate that the iron atom remains in the ferric low-spin state and also that coordination to the protein thiolate is probably maintained during the course of the heme group modification (*16*, *17*). High-spin ferric P450 complexes, for example, are characterized by rhombic EPR signals with *g*-values of ~8, 4, and 1.8 (*18*). Furthermore, a change in the axial ligand upon formation of this intermediate would likely result in a more profound change in the EPR spectrum. Sono et al. (*19*) and Sono and Dawson (*20*), using a variety of external ligands, showed that the *g*-values for ferric low-spin cytochrome P450 complexes all fall within a relatively narrow range (2.49−1.92). In contrast, heme-containing enzyme complexes in which nitrogen atoms occupy the fifth coordination site (i.e., myoglobin) have a broader range of *g*-values (2.63−1.78).

As the modification reaction proceeded to completion, the EPR spectrum began to strongly resemble that of the resting form of the enzyme. Once again, it can be concluded that although the heme had been chemically altered, the iron remained coordinated to the cysteine thiolate, and the enzyme remained in the low-spin form. This is also consistent with the observed shift (to 460 nm) in the Soret peak for the reduced − CO spectrum of the modified forms, since the characteristic spectral shift of the Soret peak in P450 enzymes upon CO binding has been attributed to the electron-donating properties of the cysteine thiolate ligand (*21*).

An interesting feature of these spectra is that the low-field component of the signal was split into two peaks in the presence of aldehyde; it became a single peak in the intermediate and either returned to a double peak (with 3PP) or became a triple peak (with 3PB). The initial appearance of the signal at $g = 2.44$ was likely due to the formation of a complex between the aldehyde substrate and heme iron. LeLean et al. (*22*) recently reported the EPR spectra for the 3PP and cyclohexanecarboxaldehyde complexes of P450$_{2B4}$(Δ2−27), which indicated similar shifts in the low-field component on aldehyde binding. The presence of two distinct signals in BM3-F87G may simply indicate incomplete binding of the aldehyde under these conditions.

The intermediate spectrum had a single low-field signal at $g = 2.39$, suggesting that the aldehyde no longer was influencing the axial symmetry of the complex. Figure 8 shows the suggested mechanism for this reaction, modified in such a way as to account for the EPR data. In particular, species b is the proposed isoporphyrin complex that corresponds to the spectral intermediate reported here. According to this mechanism, the deformylation of the parent aldehyde results in the generation of a ferric−hydroxy porphyrin complex in which the resulting alkyl radical has recombined with the porphyrin π-cation radical to produce an alkylated heme, in which the γ-meso carbon has a distorted tetrahedral geometry. The component of the signal centered at $g = 2.25$ in the resting enzyme was shifted to 2.21 in the intermediate spectrum, consistent with a distortion of the ligand field

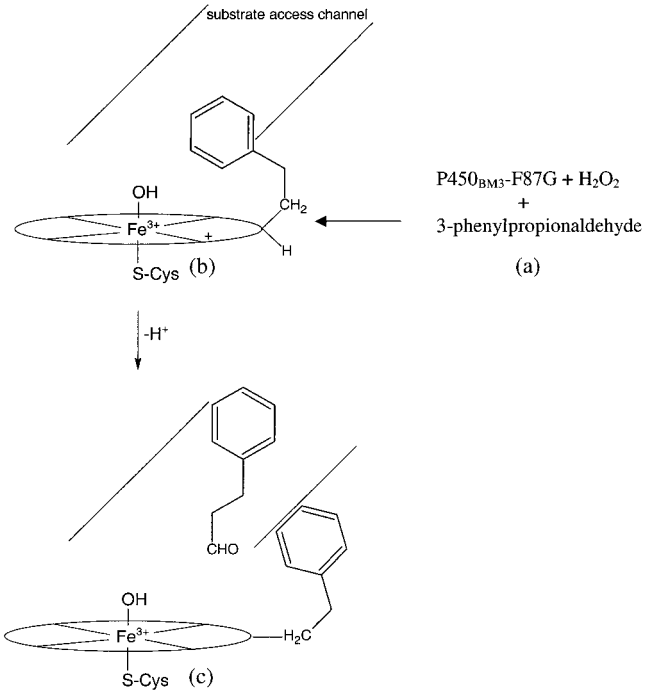

FIGURE 8: Proposed mechanism for the modification of the heme prosthetic group of $P450_{BM3}$-F87G in a reaction involving hydrogen peroxide and 3PP.

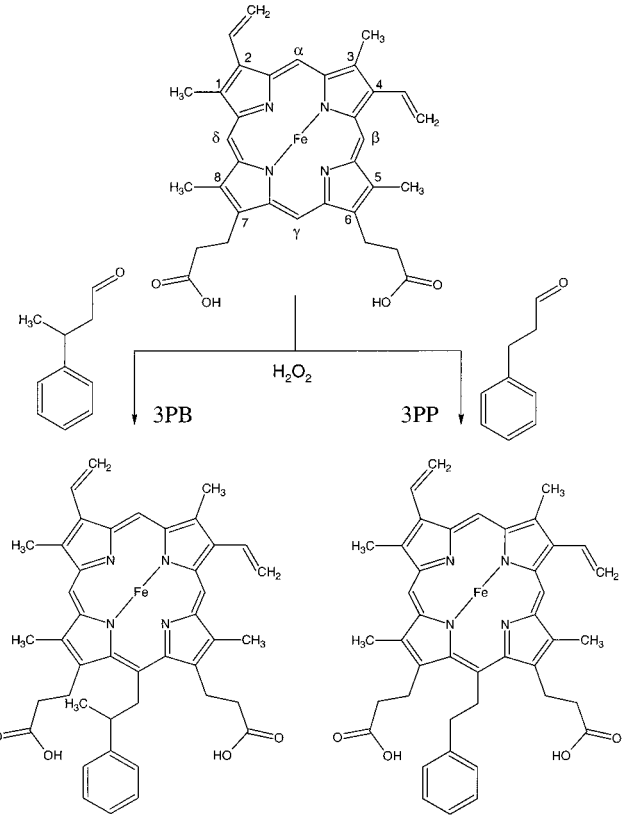

FIGURE 9: Proposed structures of the heme adducts generated in the H_2O_2-dependent reactions of 3-phenylpropionaldehyde and 3-phenylbutyraldehyde with BM3-F87G.

associated with the porphyrin pyrrole nitrogens. This distortion could easily be rationalized in terms of an sp^3-hybridized carbon in the meso position of the porphyrin, as proposed.

The bonding geometry at the γ-meso carbon would allow the phenyl ring from the attached phenylethyl group to extend above the plane of the porphyrin and effectively close off the substrate access channel, thus preventing additional aldehyde binding to the metal center. As the reaction proceeds, the aromatization of the porphyrin ring, with loss of a proton, pulls the phenylethyl group down toward the plane of the macrocycle allowing additional aldehyde to bind, resulting in splitting of the low-field signal.

It was previously assumed (*4*) that the modification of the heme occurred at a meso position of the porphyrin ring on the basis of comparisons with the rabbit liver 2B4 isoform. In studies by Kuo et al. (*8*) it was shown that aldehydes could be activated by $P450_{2B4}$ in one of two ways, both of which resulted in heme adduct formation. The first involved a putative oxenoid iron intermediate and the generation of an aldehyde-derived alkoxy radical, which added to the porphyrin γ-meso carbon. The second was believed to occur via a peroxide-dependent mechanism, resulting in deformylation of the aldehyde and alkyl radical addition to the γ-meso heme position. The two types of adducts could be distinguished on the basis of the wavelength maximum of their Soret peaks. In the current study involving $P450_{BM3}$-F87G, the heme adducts were clearly of the second type, with Soret peaks at 408 nm, and mass spectral analysis of the F87G-3PP heme confirmed addition of a phenylethyl group (104 Da) to the heme. The X-ray crystal structure of the BM3 enzyme and the positioning of the Phe side chain in the wild-type enzyme, relative to the heme, argue for the attack occurring at the γ-meso position in BM3-F87G. However, the previous study on BM3-F87G did not directly address the regioselectivity of the alkylation.

In an attempt to confirm the position of alkyl group attachment, the heme adduct formed in the reaction of $P450_{BM3}$-F87G with 3PP was examined using 1D and 2D NMR. The presence of three meso proton signals in the 1D spectrum indicated that the initial assumption in which modification had occurred at a meso position was correct. The specific meso position where the modification occurred was determined by assigning each of the remaining meso proton signals. The observed NOEs between the signal at 9.71 ppm and two different methyl protons clearly identified it as the δ-meso proton, as this is the only position capable of interacting with two methyl groups. The remaining two meso protons, at 9.89 and 9.98 ppm, showed NOE interactions with one methyl proton each. Since the α- and β-protons each lie in the vicinity of a single methyl group, we conclude that the modification by 3PP occurred at the γ-meso position (Figure 9). To assign the α- and β- protons, additional NOE interactions were examined.

The α-propionic acid protons interacted with the methyl protons at 3.43 and 3.46 ppm, which identified these groups as the 5- and 8-methyls, respectively. The methyl protons at 3.46 also interacted with the δ-meso proton, indicating that this signal could be assigned to the 8-methyl protons. The peak at 3.43 ppm was then assigned to the 5-methyl protons. Since the 5-methyl protons would be expected to show an interaction with the β-meso proton, we could assign the signal at 9.89 ppm to the β-meso proton. The remaining meso proton signal at 9.98 ppm, therefore, was assigned to the α-meso proton. These values agree very well with those reported by Kuo et al. (*8*). However, in the current study, we do not observe methyl peaks at 3.74 and 3.29 ppm as

reported in the previous study. Rather, a single peak at 3.57 ppm that integrated as six protons appeared to represent the remaining two methyl groups. This signal also appeared in the previously reported spectrum for the 3PP-modified heme in 2B4 but was not assigned. The NOE data shown here clearly indicate that these methyl groups interacted with the δ-meso or α-meso protons, consistent with their identification as the 1- and 3-methyl groups.

The 1D spectrum of the 3PB-modified heme was much more complicated. Two of the meso proton signals appeared to be doublets, but all three integrated as single protons. Many other proton signals appeared to be split in a similar fashion, suggesting that there were two structurally similar, but not identical, molecules present in the sample. The parent aldehyde, in this case, 3PB, had a chiral center at the β-carbon, and the sample used to generate the heme adduct was a mixture of the two enantiomers. It is therefore likely that there was no stereochemical selectivity for either of the isomers in this modification reaction, since both appeared to be equally represented in the product heme. Peak assignments were made using NOE data, as with the 3PP sample. The singlet signal at 9.97 ppm and the doublet centered at 9.94 ppm were assigned to the α- and β-protons. It was not possible with this sample to distinguish these protons from one another due to the complexity of the spectrum. The doublet centered at 9.75 was assigned to the δ-meso proton because of its interaction with two different methyl signals. Once again, the only signal missing was the γ-meso proton, indicating that 3PB modified the heme at the γ-meso position.

It should also be noted that in the 3PB-modified heme the chiral carbon was well removed from the porphyrin ring system and would not be expected to cause large changes in the chemical shifts through scaler coupling interaction. For example, six bonds separated the chiral carbon from either the δ- or β-positions on the modified heme, yet one or both of these signals appeared as a doublet, indicating the stereochemistry of the chiral carbon had far-reaching effects. One explanation for this is that steric crowding in the vicinity of the propionate groups caused a distortion of the planar heme, and the distortion was sensitive to the stereochemistry of the attached chiral carbon. Alternatively, the phenyl ring of the attached alkyl substituent may lie to one side of the heme or the other (i.e., closer to the β-meso hydrogen in one isomer and closer to the δ-meso hydrogen in the other), depending on the isomeric form of the aldehyde involved. The corresponding ring currents associated with the phenyl group could then alter the chemical shifts of protons that lie above or below it.

An additional signal was observed in the 3PB-heme spectrum at -1.20 ppm that was not observed for the 3PP-heme. The signal integrated as three protons and appeared as a doublet. Given the splitting of most of the proton signals in the 3PB spectrum, it could easily be viewed as two separate singlet peaks, which would be consistent with its assignment to the branching methyl group on the attached phenylisopropyl group. The upfield shift suggests that the methyl group was positioned above the planar ring system of the heme.

Heme adduct formation is not uncommon in P450 catalysis, as the catalytic cycle is known to generate highly reactive intermediates, which in turn can react with substrates to produce mobile reactive species with access to sites around the porphyrin ring system. The reaction of these aromatic aldehydes in BM3-F87G is unusual in that it is highly regiospecific and results in a stable, intact enzyme that appears capable of accepting electrons from NADPH and carrying out substrate oxidations. Generally, when protein adduct formation is described, it refers to a destructive process that abolishes catalytic activity, so the resulting enzyme is of little or no value for subsequent mechanistic studies. This is the case with N-alkylated hemes generated in the reactions of ethylene (*23*), TTMS (*24*), 5-phenylpentyne (*25*), and a variety of other compounds (*26*, *27*) with microsomal cytochrome P450.

The 3PP- and 3PB-modified forms of the enzyme were both shown to be capable of accepting electrons from NADPH as determined using stopped-flow NADPH consumption assays with lauric acid as the substrate. In fact, attachment of the alkyl group to the γ-meso position of BM3-F87G had very little effect on the rate at which electrons were transferred from NADPH. However, whereas BM3-F87G was less active than wild type in the hydroxylation of lauric acid, the F87G-3PP and F87G-3PB forms showed no activity at all. This is in contrast to the NADPH oxidation results indicating that both modified forms were approximately equal to F87G in their activity. One likely explanation is that the modified enzymes utilize the electrons from NADPH in an unproductive manner, such as the formation of H_2O_2 or superoxide from O_2. Why these enzymes are incapable of inserting oxygen into the substrate is unclear; however, the activation energy required to cleave an unactivated C$-$H bond is considerable. One possible explanation is that the activated P450 intermediate in the modified enzymes is not a sufficiently strong oxidizing agent to carry out the initial hydrogen abstraction necessary to catalyze the reaction. This may also be the case with Mn-substituted P450$_{CAM}$, in which iodosobenzene can serve as an oxygen atom donor to produce the Mn(V)$=$O complex, but this activated form of the enzyme is more stable than the analogous iron complex and cannot readily abstract a hydrogen atom from camphor (*28*). Alternatively, the attached alkyl groups may somehow sterically hinder the substrate lauric acid from penetrating the active site.

To explore these possibilities further, two aromatic substrates, 4-nitrophenol and 4-nitrocatechol, were chosen as probes for P450 catalytic activity. In the reactions involving 4-nitrocatechol oxidation, the activities of the wild-type, F87G, F87G-3PP, and F87G-3PB enzymes were comparable. The effect of SOD and glutathione on this reaction indicated that hydroxylation occurred due to the uncoupled oxidation of NADPH and generation of superoxide. In contrast, 4-nitrophenol oxidation was clearly not the result of NADPH uncoupling, as neither SOD nor catalase had a significant effect on product formation. In addition, substrate binding as reflected by K_m for the wild-type enzyme was much weaker than for the F87G mutant, which is consistent with this oxidation occurring in the active site, since the F87G mutant is known to better accommodate aromatic substrates.

It is difficult to rationalize the low K_m values associated with the modified enzymes since the modification is expected to replace the bulky phenyl ring that was removed from the wild-type enzyme through mutagenesis, which could effect substrate binding. However, the K_m and V_{max} values obtained

for these reactions were based on an approximation of linearity for the initial 10 s of the reaction, and as indicated previously, the modified forms appear to be more susceptible to turnover-dependent inactivation. This could have the effect of artificially lowering both the K_m and V_{max} values. Still, it is clear that both modified enzymes retained significant activity in the hydroxylation of 4-nitrophenol, yet were incapable of hydroxylating lauric acid.

We offer two possible explanations for these findings: first, the lack of activity with lauric acid may be the result of the substrate's inability to bind effectively to the modified enzymes. On the other hand, the binding of 4-nitrophenol may be affected to a much lesser degree. Alternatively, the difference in activities may result from differences in the catalytic mechanism involved in the oxidation of these two types of substrates. It is widely accepted that hydroxylation of many aromatic substrates by cytochrome P450 occurs via an epoxide intermediate, rather than hydrogen atom abstraction. This mechanism has been used to explain the "NIH shift" that has been observed with certain substituted aromatic substrates (*29*, *30*). Structure−activity studies involving the hydroxylation of monohalogenated benzenes by P450 further suggest that epoxide formation may occur via an initial one-electron transfer from the substrate to the activated intermediate, followed by the transfer of an oxygen (*31*). The activation barrier for electron transfer in these aromatic-type substrates would be expected to be much lower than for abstraction of a hydrogen atom from an aliphatic substrate. It could therefore be argued that the stability of the activated species in the covalently modified enzymes is enhanced due to the presence of the attached alkyl groups, and consequently, they are thermodynamically incapable of abstracting a hydrogen atom from lauric acid. This would also be consistent with the reduction in 4-nitrophenol hydroxylation activity observed with the modified forms, although steric effects could also account for this. Furthermore, Ortiz de Montellano et al. have shown that, for reactions involving electron transfer, the heme edge may be the site of contact between the activated intermediate and the substrate in horseradish peroxidase (*32*). In this case, the oxo group is not accessible by the substrate. Perhaps the modification of the heme in $P450_{BM3}$-F87G precludes the binding of substrate near the oxene, whereas 4-nitrophenol oxidation does not require this direct contact.

Although we cannot fully explain the differences in catalytic activities of the modified $P450_{BM3}$-F87G derivatives toward lauric acid and 4-nitrophenol, it is clear that covalent modification of the heme prosthetic group in cytochrome $P450_{BM3}$-F87G occurs only at the γ-meso position via formation of a thiolate-bound isoporphyrin species, and this modification does not fully destroy the enzyme's catalytic potential. Rather, the activity of the enzyme is altered, such that certain substrates can no longer be oxidized, while the activity toward other substrates is affected to a relatively small degree. We suggest that either steric or electronic factors, or more likely a combination of both, account for these differences.

ACKNOWLEDGMENT

We thank Dr. Nadja Cech (The University of North Carolina at Greensboro) for assistance in acquiring mass spectral data.

REFERENCES

1. White, I. N. H. (1982) *Chem.-Biol. Interact. 39*, 231−243.
2. Raner, G. M., Vaz, A. D. N., and Coon, M. J. (1996) *Mol. Pharmacol. 49*, 515−522.
3. Raner, G. M., Chiang, E. W., Vaz, A. D. N., and Coon, M. J. (1997) *Biochemistry 36*, 4895−4902.
4. Raner, G. M., Hatchell, J. A., Morton, P. E., Ballou, D. P., and Coon, M. J. (2000) *J. Inorg. Biochem. 81*, 153−160.
5. Wiseman, J. S., Nichols, J. S., and Kolpak, M. X. (1982) *J. Biol. Chem. 257*, 6328−6332.
6. Ator, M. A., David, S. K., and Ortiz de Montellano, P. R. (1989) *J. Biol. Chem. 264*, 9250−9257.
7. Choe, Y. S., and Ortiz de Montellano, P. R. (1991) *J. Biol. Chem. 266*, 8523−8530.
8. Kuo, C.-L., Raner, G. M., Vaz, A. D. N., and Coon, M. J. (1999) *Biochemistry 38*, 10511−10518.
9. Graham-Lorence, S., Truan, G., Peterson, J. A., Falck, J. R., Wei, S., Helvig, C., and Capdevila, J. (1997) *J. Biol. Chem. 272*, 1127−1135.
10. Schwaneberg, U., Schmidt-Dannert, C., Schmitt, J., and Schmid, R. D. (1999) *Anal. Biochem. 269*, 359−366.
11. Li, Q. S., Schwaneberg, U., Fischer, P., and Schmid, R. D. (2000) *Chem. Eur. J. 6*, 1531−1536.
12. Carmichael, A. B., and Wong, L. L. (2001) *Eur. J. Biochem. 268*, 3117−3125.
13. Omura, T., and Sato, R. (1964) *J. Biol. Chem. 239*, 2379−2385.
14. Larson, J. R., Coon, M. J., and Porter, T. D. (1991) *Proc. Natl. Acad. Sci. U.S.A. 88*, 9141−9145.
15. Dawson, J. H., Andersson, L. A., and Sono, M. (1982) *J. Biol. Chem. 257*, 3606−3617.
16. Dawson, J. H., and Sono, M. (1987) *Chem. Rev. 87*, 1255−1276.
17. Sono, M., Roach, M. P., Coulter, E. D., and Dawson, J. H. (1996) *Chem. Rev. 96*, 2841−2887.
18. Collman, J. P., Sorrell, T. N., and Hoffman, B. M. (1975) *J. Am. Chem. Soc. 97*, 913−914.
19. Sono, M., Andersson, L. A., and Dawson, J. H. (1982) *J. Biol. Chem. 257*, 8308−8320.
20. Sono, M., and Dawson, J. H. (1982) *J. Biol. Chem. 257*, 5496−5502.
21. Hanson, L. K., Eaton, W. A., Sligar, S. G., Gunsalus, I. C., Gouterman, M., and Connell, C. R. (1976) *J. Am. Chem. Soc. 98*, 2672−2674.
22. LeLean, J. E., Moon, N., Dunham, W. R., and Coon, M. J. (2000) *Biochem. Biophys. Res. Commun. 276*, 762−766.
23. Ortiz de Montellano, P. R., Beilan, H. S., Kunze, K. L., and Mico, B. A. (1981) *J. Biol. Chem. 256*, 4395−4399.
24. Kimmett, S. M., Whitney, R. A., and Marks, G. S. (1996) *Mol. Pharmacol. 49*, 676−682.
25. Roberts, E. S., Alworth, W. L., and Hollenberg, P. F. (1998) *Arch. Biochem. Biophys. 354*, 295−302.
26. Estefania, L.-C., He, K., Yin, H., and Correia, M. A. (1997) *Arch. Biochem. Biophys. 338*, 35−42.
27. Osawa, Y., Fellows, C. S., Meyer, C. A., Woods, A., Castoro, J. A., Cotter, R. H., Wilkins, C. L., and Highet, R. J. (1994) *J. Biol. Chem. 269*, 15481−15487.
28. Gelb, M. H., Toscano, W. A., Jr., and Sligar, S. G. (1982) *Proc. Natl. Acad. Sci. U.S.A. 79*, 5758−5762.
29. Jerina, D. M., and Daly, J. W. (1974) *Science 185*, 573−582.
30. Koerts, M., Soffers, A. E., Vervoort, J., DeJager, A., and Rietjens, I. M. (1998) *Chem. Res. Toxicol. 11*, 503−512.
31. Burka, L. T., Plucinski, T. M., and Macdonald, T. L. (1983) *Proc. Natl. Acad. Sci. U.S.A. 80*, 6680−6684.
32. Ortiz de Montellano, P. R., Choe, Y. S., DePillis, G., and Catalano, C. E. (1987) *J. Biol. Chem. 262*, 11641−11646.

BI020256C